FACTA UNIVERSITATIS
Series: **Mechanical Engineering** Vol. 22, Nº 4, 2024, pp. 615 - 632
https://doi.org/10.22190/FUME240920049M

Original scientific paper

COMPARISON OF THE EFFECT OF ELECTROPLASTICITY IN COPPER AND ALUMINUM

Alina Y. Morkina[1,2], Danila V. Tarov[2], Gulnara R. Khalikova[1,3], Alexander S. Semenov[4], Pavel S. Tatarinov[4], Ilya A. Yakushev[4], Sergey V. Dmitriev[1,3]

[1]Institute for Metals Superplasticity Problems of Russian Academy of Sciences, Ufa, Russia
[2]Research Laboratory for Metals and Alloys under Extreme Impacts, Ufa University of Science and Technology, Ufa, Russia
[3]Ufa State Petroleum Technological University, Ufa, Russia
[4]Polytechnical Institute (branch) in Mirny, North-Eastern Federal University, Mirny, Russia

ORCID iDs: Alina Y. Morkina https://orcid.org/0000-0002-3989-0376
Danila V. Tarov https://orcid.org/0009-0009-4539-1248
Gulnara R. Khalikova https://orcid.org/0000-0002-6712-8469
Alexander S. Semenov https://orcid.org/0000-0001-9940-3915
Pavel S. Tatarinov https://orcid.org/0000-0001-7430-8591
Ilya A. Yakushev https://orcid.org/0000-0003-2539-7334
Sergey V. Dmitriev https://orcid.org/0000-0002-6744-4445

Abstract. *The effect of electroplasticity (EE) is used to increase the deformability of metals and alloys, save the energy used to deform them, and reduce tool wear. Despite the practical importance of EE, there is no consensus in the literature on its physical nature, and further research is needed to elucidate it. In this work, the tensile deformation of aluminum and copper wires stimulated by the repetitive electric pulses is experimentally investigated. Copper and aluminum have low and high stacking fault energy, respectively, and it is interesting to compare the behavior of these metals during electrically assisted plastic deformation. Joule heat release is precisely controlled in the experiments. Both metals show qualitatively similar behavior, with the increment in plastic deformation decreasing with pulse number at fixed tensile stress. This result supports the dislocation mechanism of EE in these metals.*

Key words: *Effect of electroplasticity, Tensile deformation, Copper, Aluminum, Creep, Current pulses*

Received: September 20, 2024 / Accepted November 20, 2024
Corresponding author: Sergey V. Dmitriev
Institute for Metals Superplasticity Problems of RAS, Khalturin St. 39, 450001 Ufa, Russia
E-mail: dmitriev.sergey.v@gmail.com

1. INTRODUCTION

Troitskii first identified the effect of electroplasticity (EE) in metals in 1969 [1], and subsequent research has extensively explored this phenomenon through numerous studies [2]. The effect is the reduction in yield stress when high-density electric current pulses are applied to metallic materials. The temperature increase in the deformed material can be relatively small, and Joule heating alone is insufficient to account for the significant increase in plasticity observed. As a result, the energy-saving approach to metal forming can be developed with the help of EE. The ability to form parts with minimal heating allows for more energy efficient manufacturing processes, reducing overall energy consumption. In recent years, studies on EE have gained considerable attention due to its usefulness in a wide range of industrial sectors [3-5]. Due to the skin effect [6,7], EE can be observed only in relatively thin workpieces during rolling [8,9], drawing [10-13], stamping [14,15], cutting [16], forging [17,18], and forming [5,6,19-23].

At the same time, the fundamental principles and mechanisms underlying EE remain not fully understood. Researchers have consistently pointed to two key mechanisms responsible for EE: non-uniform Joule heat release and electron wind action [24-26]. Although the heat released at defects such as dislocations and grain boundaries increases their mobility and enhances ductility, the overall increase in average temperature remains negligible. In addition, the electron wind exerts a force on the dislocations, which also contributes to the increase in their mobility. Experimental studies have provided evidence supporting the electron wind theory as an explanation for EE [26]. However, one study [27] observed non-directional migration of twin boundaries in response to electropulsation, which was attributed to the interaction between electrons and dislocations rather than the electron wind force. The mechanisms of EE have been discussed in several research and review articles [28-31].

In recent years, research has been conducted to gain a deeper understanding of EE and to explore its potential applications in the processing of various metallic materials. A method for self-healing of metallic materials using pulsed electric current to restore the microstructure has been developed [32]. The research by Kim et al. [33] showed that the application of electric current during tensile testing of an Al-Mg-Si alloy can induce structure relaxation and void formation processes. Lahiri et al. selected various parameters that affect the reduction of flow stress during electropulsation to explain the mechanism of electroplasticity in terms of crystal plasticity [34]. EE can improve the ductility of a Mg-Nd-Zn-Zr alloy [35] and hcp metals [36,37]. The effect of strain rate on plasticity and microstructure was investigated in the context of electrically assisted tensile testing of the aluminum alloy 5754-H111 [38]. The influence of microstructure on EE has been investigated in an aluminum alloy [39]. Pulsed electric current has been used to improve the formability of the 5052-H32 aluminum alloy [40]. High-density pulsed electric current is able to induce precipitation hardening of steel [41], assist the deformation of the Haynes 230 alloy [42] and the Invar 36 alloy [43]. The EE was studied in a high entropy alloy under uniaxial tension, where the study [44] reported a decrease in yield stress and an increase in strain with increasing current density. In the study [45], the effect of the angle between the direction of the applied load and the electric pulse current on the EE in the Ti-6Al-4V alloy was investigated. Increased plasticity in monatomic metallic glasses was observed when electric pulses were applied, as reported in [46]. The in-situ study of

individual dislocation motion was carried out in single crystal nickel and copper under combined electromechanical actuation as reported in [47] and [48], respectively.

The loading scheme can strongly influence the development of plastic flow in metals [49,50] and thus the manifestation of EE [51-56]. In the present study, EE is studied for copper and aluminum wires under tensile loading. There are two main goals of this work. First is to assess the effect of multiple electric pulses at fixed tensile stress. Joule heat release does not depend on the pulse number and if the deformation increment will also be same for each current pulse, this would suggest that the observed plastic deformation is related to the temperature increase of the wire. On the other hand, if EE is realized through the depinning of dislocations, then the increment of plastic deformation is expected to reduce from pulse to pulse, as dislocations will eventually pinned by stronger obstacles. The observation that the deformation increment decreases with increasing pulse number under constant stress was reported in [57] for nanoindentation and compression. The second goal is to compare EE in two metals with significantly different stacking fault energy. Copper and aluminum have considerably different values of the stacking fault energy, about 0.04 and 0.2 J/m^2, respectively [58-60]. As the results, twins are easily formed in copper but not in aluminum. If a difference in the behavior of copper and aluminum will be observed, this would reveal the contribution of twins to EE, otherwise, in both metals EE is realized through the activation of dislocation motion. In our previous study [61] the effect of several high-density electric current pulses on the deformation of copper wires in different structural states under tension was investigated. In this work, a comparison between the uniaxial tension of copper and aluminum wires under the action of repetitive electric pulses is carried out.

Additionally, the cooling time of the samples after several pulses at different applied voltages was examined.

2. MATERIALS AND METHODOLOGY

2.1. Microstructure Characterization

In this work, copper and aluminum wires of M1 and KAS 8176 grades, respectively, are used as samples. The chemical composition of the metals studied is given in Tables 1 and 2, respectively. The choice of these materials is based on their use in the production of electrical wires by drawing, and this process can be improved by EE. It is also interesting to compare these metals because, as mentioned in the introduction, there is a significant difference in the values of the stacking fault energy in copper and aluminum. Samples with a length of 360 mm were obtained from copper (aluminum) wire with a cross-sectional diameter of 1 mm (1.79 mm).

The wires were examined in their as-received condition and after annealing to a larger grain size. Copper wire was annealed at 500°C for 2 hours and oven cooled, and aluminum wire was annealed at 450°C for 2 hours and oven cooled.

Table 1 Chemical composition of grade M1 copper

Mass fraction of element										
Cu	Impurities, no more									
no less	Bi	Fe	Ni	Zn	Sn	Sb	As	Pb	S	O
99.90	0.001	0.005	0.002	0.004	0.002	0.002	0.002	0.005	0.004	0.05

Table 2 Chemical composition of KAS 8176 aluminum

Mass fraction of element										
Al	Impurities, no more									
no less	Si	Fe	Cu	Mn	Mg	Cr	Ni	Zn	Ti	Ga
99.35	0.03-0.15	0.40-0.15	-	-	-	-	-	0.10	-	-

The surface of specimens for EBSD analysis was prepared as follows: material blanks were cut into plates by electrospark method, then these plates were mechanically thinned on abrasive paper with gradual reduction of abrasive value, then polishing was carried out on diamond paste also with gradual transition to finer abrasive. The final polishing was carried out by jet electropolishing on the "Tenupol - 3" machine using electrolyte of the following composition: for copper wire 20% aqueous solution of H_3PO_4 (at room temperature), for aluminum wire 750 ml methanol, 250 ml HNO_3 (at 28°C). The polishing time was 20 sec.

EBSD (Electron Back Skatter Diffraction) analysis was performed on a TescanMira 3LMH scanning electron microscope using the built-in "CHANNEL 5.0" software. Imaging was performed at an accelerating voltage of 20 kV. For all states, the imaging step was set to 0.5 μm for copper wire and 0.3 μm for aluminum wire, with a maximum allowable misorientation error of 2°. The number of Kikuchi lines used to index the diffraction patterns was at least 5. To increase the reliability of the EBSD data obtained in the analysis of crystallographic grain misorientation, regions consisting of five points or less were removed from the EBSD maps as unreliable [62]. The resulting misorientation maps show the different crystallographic orientations in different colors. Boundaries with misorientations between 2 and 15° were considered low-angle boundaries (LABs), and those with misorientations greater than 15° were considered high-angle boundaries (HABs), with twin boundaries labeled Σ3. Structures were analyzed quantitatively according to ASTME112-10 recommendations. The equivalent diameter was used as the grain size.

The EBSD inverse pole figure (IPF) map and corresponding misorientation angle distributions for copper and aluminum wires in the as-received condition are shown in Figs. 1 and 2, while similar plots for the annealed copper and aluminum wires are shown in Figs. 3 and 4. The left (right) columns in these figures show the results for the cross sections along (normal to) the wire axis. It can be seen from Figs. 1 and 2 that the structure in the as-received wires is recrystallized with random orientation of the grains in the longitudinal direction and preferential <111> orientation in the transverse direction for copper and <111> + <100> for aluminum. The ratio of twin boundaries for copper wire reaches 0.53 for as-received and 0.81 for annealed wires (see Figs. 1 and 3). The average grain size for as-received copper wire, excluding twin boundaries, is 9.1 ± 0.4 μm and 8.2 ± 0.2 μm in the longitudinal and transverse directions, respectively (Fig. 1). For as-received aluminum wire, the grain sizes are 7.6 ± 0.3 μm and 6.2 ± 0.2 μm in the longitudinal and normal directions, respectively (Fig. 2). The grain size in copper increases significantly after annealing, up to 113.8 μm for the longitudinal and 50.4 μm for the normal cross section (Fig. 3). In contrast, the grain size in annealed aluminum increases only slightly to 12.3 ± 0.3 μm and 6.2 ± 0.2 μm for the longitudinal and normal cross sections, respectively (Fig. 4).

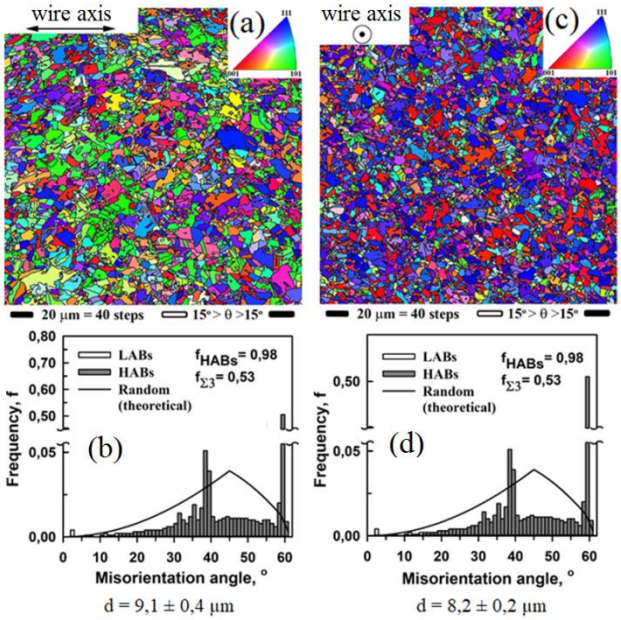

Fig. 1 The microstructure of the as-received copper wire: (a,c) grain orientation distribution maps, (b,d) grain boundary distribution according to misorientation angle. Results for section (a,b) along the wire axis and (c,d) normal to the wire axis

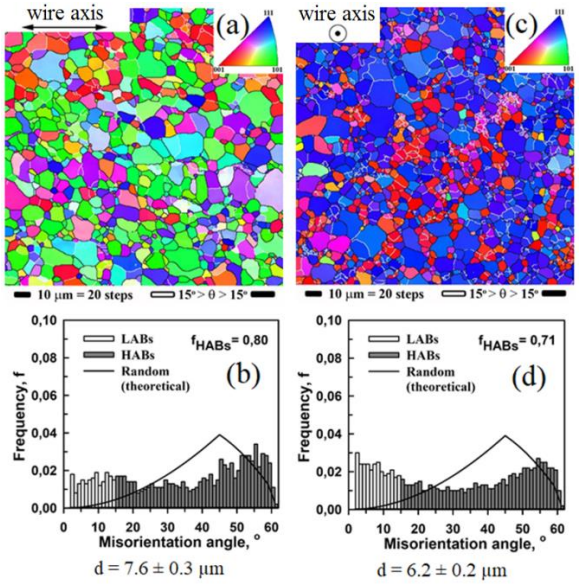

Fig. 2 The microstructure of the as-received aluminum wire: (a,c) grain orientation distribution maps, (b,d) grain boundary distribution according to misorientation angle. Results for section (a,b) along the wire axis and (c,d) normal to the wire axis

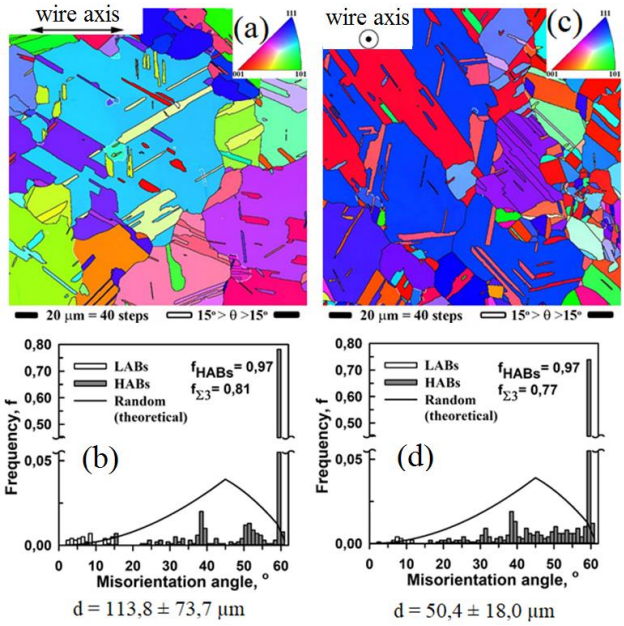

Fig. 3 The microstructure of the annealed copper wire: (a,c) grain orientation distribution maps, (b,d) grain boundary distribution according to misorientation angle. Results for section (a,b) along the wire axis and (c,d) normal to the wire axis

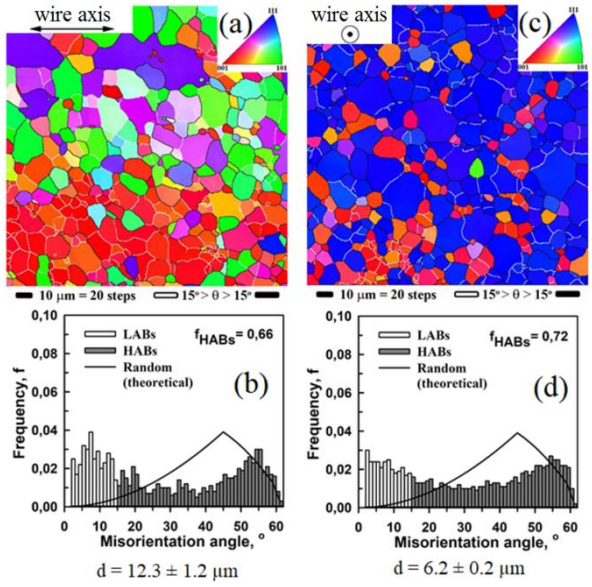

Fig. 4 The microstructure of the annealed aluminum wire: (a,c) grain orientation distribution maps, (b,d) grain boundary distribution according to misorientation angle. Results for section (a,b) along the wire axis and (c,d) normal to the wire axis

In summary, copper contains a large number of twins, while twins are almost absent in aluminum, which is a consequence of the large difference in stacking fault energy between these metals. It is also important to note that the grain size of the annealed copper is an order of magnitude larger than that of the as-received copper, whereas the grain size of the aluminum wires is only slightly increased by annealing.

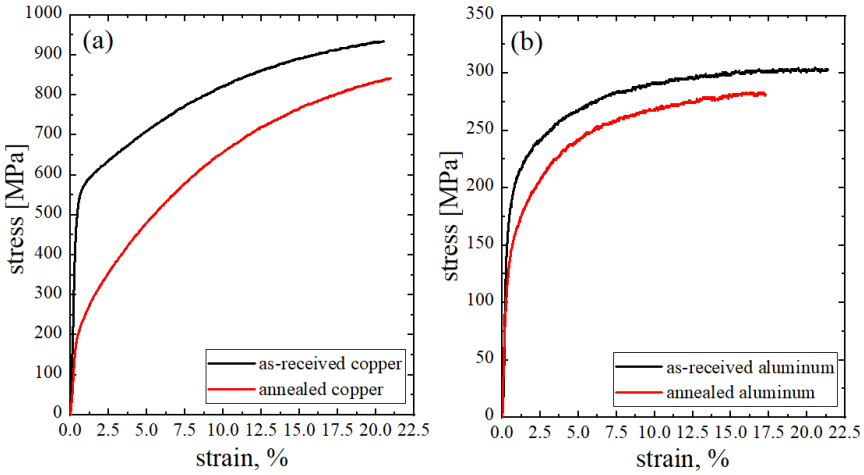

Fig. 5 Stress-strain curves for as-received (black) and annealed (red) specimens deformed at a strain rate of 1.1×10^{-3} s^{-1}: (a) copper and (b) aluminum

2.2. Stress-Strain Curves

Tensile tests were performed on long copper and aluminum wires (360 mm) at room temperature. The tests were performed using a Schenck Trebel RMC100 universal electromechanical machine with a force of 100 kN. Figure 5 shows the stress-strain curves for copper and aluminum, with the black curves representing the initial condition and the red curves representing the annealed condition.

It can be seen that for both metals the stress levels required for deformation are lower in the annealed condition. This is particularly noticeable in the case of copper, where there is a large difference in grain size between the annealed and as-received specimens, while for aluminum this difference is small.

According to the results obtained, the yield stresses of copper and aluminum in both structural states were determined. The yield stress of copper (aluminum) in the initial state is 125 MPa (55 MPa), and after annealing it is 95 MPa (45 MPa). Based on these values, the tensile stress in the EE experiments was selected.

3. Results

3.1. Joule Heat Release

A detailed description of the experimental setup and methodology is given in our previous study [61].

First, the Joule heat release on the samples due to a current pulse from a battery of capacitors charged to different voltages is measured. The dead load is chosen to be 65 N, which corresponds to a tensile stress of 83 MPa for copper and 26 MPa for aluminum. In both cases, the specimens are loaded in the elastic region. The voltage range of the capacitor bank is varied from 45 to 100 V in 5 V steps. After each current pulse, the tensile strain of the specimen associated with thermal expansion, $\Delta\varepsilon_J$, is measured and the increase in temperature is calculated using the formula

$$\Delta T = \frac{\Delta\varepsilon_J}{\alpha}, \tag{1}$$

where the coefficient of thermal expansion α at room temperature is 16.9×10^{-6} K^{-1} and 22.2×10^{-6} K^{-1} for copper and aluminum, respectively.

Figure 6 shows the function of temperature increase with voltage on the capacitors for copper and aluminum in two states, as-received and annealed. The results for the samples in the as-received state are indicated by black curves and for the annealed state by red curves. For better accuracy, the experiments were done twice and the results obtained were averaged. Note that the results presented in double logarithmic scale are well approximated by straight lines, implying the power dependence between ΔT and V in the form

$$\Delta T \sim V^s. \tag{2}$$

The blue dashed line in Fig. 6 has a slope of s=2.4, which is very close to the slope of the experimental curves for both metals regardless of the structural state.

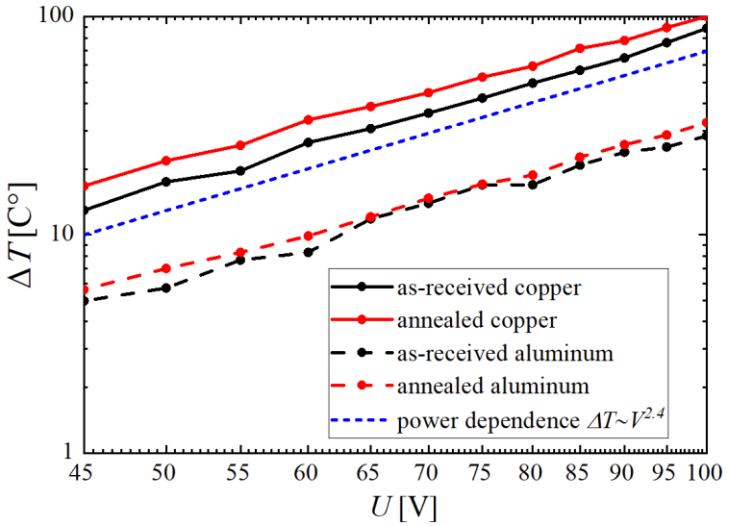

Fig. 6 Temperature increase of samples due to Joule heat release as a function of voltage across the capacitor battery for copper (solid) and aluminum (dashed) lines. Results for as-received (annealed) samples are shown in black (red). The blue dashed line shows the power dependence of ΔT on U with the exponent s=2.4. Each curve is the average of the results from two experiments

The energy stored in the capacitor is proportional to the square of the voltage, $E=CU^2/2$, where C is the capacitance of the capacitor. One could expect that the Joule heat release would also be proportional to the square of U, but the experiment showed a slightly faster growth. This can be attributed to the increased resistance of the wires as the temperature rises.

From Figure 6 it can be seen that the temperature increase of the annealed specimen is greater than that of the as-delivered specimen. This can be explained by the decrease in grain boundary density in the annealed specimens and thus the dissolution of grain boundary segregations. It is well known that elements in solid solution significantly increase the electrical resistivity of metals, resulting in an increase in the heat dissipation due to the passing current. Note that for copper, the difference in heat dissipation between annealed and as-received samples is greater than for aluminum. This is because the grain size difference between annealed and as-received copper wires is greater than for aluminum wires.

In the previous experiment for copper samples [61], the battery voltage was chosen to be 60 V, for which the wire temperature increase is about 25 K, see Fig. 6. In this study, this voltage across the capacitor is used for copper, but a different voltage is chosen for aluminum because the aluminum wire has a different cross-sectional area and different physical properties. The voltage is chosen so that the homologous temperature increase of aluminum wires is equal to that of copper wires. The melting point of M1 copper is equal to T_{m1}=1358 K and a temperature increase of 25 K corresponds to $0.0184T_{m1}$. The melting point of aluminum is T_{m2}=933 K, and $0.0184T_{m2}$=17.2 K. Approximately this heating occurs when a current pulse is applied with a battery voltage of 75 V, and this voltage is chosen in experiments with aluminum wires.

In the previous experiment for copper specimens [61], the battery voltage was chosen to be 60 V, for which the increase in the wire temperature is about 25 K, see Fig. 6. In this study this voltage across capacitor is used for copper but a different voltage is chosen for aluminum since the aluminum wire has different cross section area and different physical properties. The voltage is chosen such that the increase in the homological temperature of aluminum wires is equal to that of copper wires. The melting point of M1 copper is equal to T_{m1}=1358 K and an increase in temperature by 25 K corresponds to $0.0184T_{m1}$. The melting point of aluminum is T_{m2}=933 K, and $0.0184T_{m2}$=17.2 K. Approximately this heating occurs when a current pulse with a battery voltage of 75 V is applied and this voltage is chosen in the experiments with aluminum wires.

In summary, experiments are performed with copper wires at a voltage across the capacitor of 60 V and with aluminum wires at a voltage of 75 V. The temperature increase ΔT in both types of wires is 0.0184 of their homologous melting temperatures, which is approximately 25 K for copper and 17 K for aluminum.

3.2. Cooling and Creep of Wires after the Current Pulse

In the course of experiments at sufficiently high tensile stresses, the phenomenon of creep of samples after passing a current pulse was observed. It is known that the creep rate of metals depends significantly on temperature, so the question arose about the nature of the observed creep and its relation to Joule heating. To answer this question, the cooling and creep rates of the samples were studied.

To study the cooling rate of the specimens, the same tensile stresses were applied as in the experiment described in Section 3.1, namely, 83 MPa for copper and 26 MPa for aluminum; in both cases, the tensile stresses lie below the yield stress. The voltages across the capacitor bank were 60, 80, and 100 V for the copper specimens and 75, 110, and 140 V for the aluminum specimens. To improve accuracy, three experiments were made for each capacitor voltage and the data were averaged.

In the experiments, the decrease in length of the wires due to their cooling after the current pulse was recorded and recalculated into the temperature decrease using Eq. (1). Fig. 7 shows the results obtained for copper and aluminum wires, where the abscissa shows the time in seconds and the ordinate shows the temperature change of the samples in Kelvin. The black, red and blue curves correspond to the voltage on the capacitor batteries of 60 (75), 80 (110), and 100 (140) V used for the experiment with copper (aluminum) wires.

The results for copper in the as-received state and after annealing are plotted in Fig. 7(a). Exponential decrease of temperature in time can be seen as the logarithmic scale is used for the ordinate. The structural state does not noticeably affect the cooling of the samples as the difference is within the scattering range of the experimental data. It can be seen that the temperature decreases down to ΔT=10 K in 20, 30, and 45 s for the current pulse from the capacitor charged to 60, 80, and 100 V, respectively.

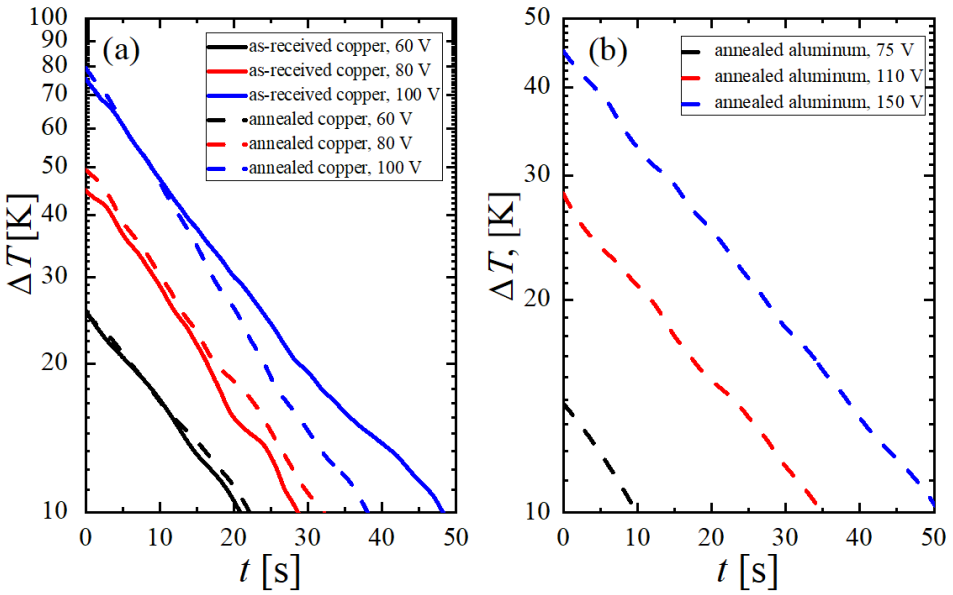

Fig. 7 Cooling rate of samples after an electric current pulse from the capacitor charge to different voltages. (a) Results for as-received (solid lines) and annealed (dashed lines) copper. (b) Results for annealed aluminum. The plots show the average result of three experiments

The cooling of the aluminum wire was measured only for the annealed sample because, as mentioned above, the grain size in the annealed and as-received aluminum samples differs not significantly, see Figs. 2 and 4. In Fig. 7(b) it can be seen that aluminum cools

down longer compared to copper and this is due to the fact that the diameter of the aluminum wire is 1.79 times larger. But even at the capacitor voltage of 150 V cooling down to ΔT=10 K takes only 50 s.

To study the creep rate, high tensile stresses of 191 MPa were chosen for the copper specimens in both structural states, and 80 and 70 MPa for the as-received and annealed aluminum specimens, respectively. The capacitor bank voltages were chosen to be 60 V for copper and 75 V for aluminum. Figure 8 shows the results for copper (aluminum) wires with solid (dashed) curves. The results for the samples in the as-received condition are shown as black curves and the results for the annealed samples are shown as red curves.

It can be seen that creep is much faster as the wire heats up after the current pulse. However, the deformation does not stop when the sample is completely cooled and continues at a slower rate. It can also be observed that the creep of the annealed specimens stops earlier compared to the original specimens. This is particularly noticeable for copper specimens.

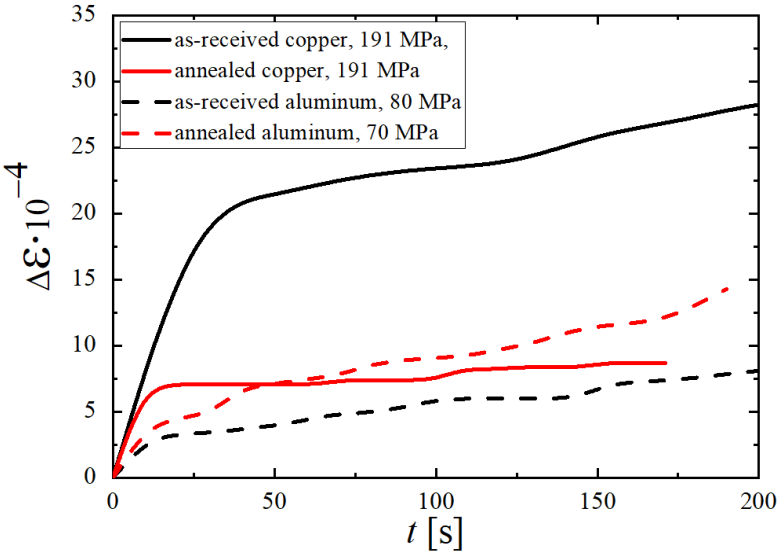

Fig. 8 Creep strain as the function of time for specimens after single electric current pulse at a fixed tensile stress for copper (solid) and aluminium (dashed) lines. Results for as-received (annealed) specimens are shown in black (red)

3.3 Wire elongation under the action of repetitive electrical pulses

The next step was to make a series of 15 current pulses with fixed tensile stress in the range of 95.5-171.9 MPa and 34-76 MPa for copper and aluminum wires, respectively. These load ranges capture the elastic and inelastic regions. Figure 9 shows the results for the specimens in the initial state, where the abscissa stands for the pulse number and the ordinate denotes the strain induced by a current pulse. Figure 9(a) shows the results for copper and (b) for aluminum.

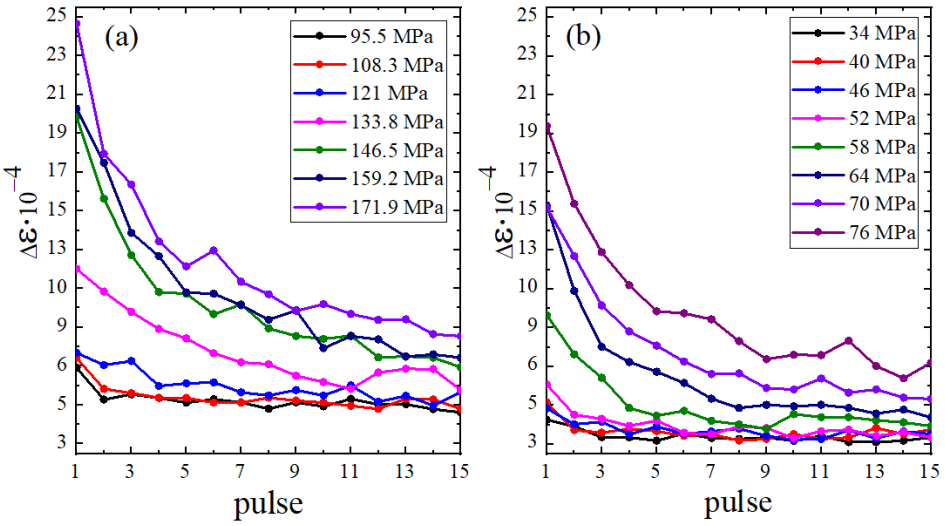

Fig. 9 The increase in plastic deformation as a function of the electric current pulse number at various values of the fixed tensile stress. Fifteen current pulses are applied for each tensile stress, after which the load is increased. Results for the as-received specimens of (a) copper and (b) aluminum. Each curve is the average of two experiments. The capacitor bank voltage is 60 V for copper and 75 V for aluminum

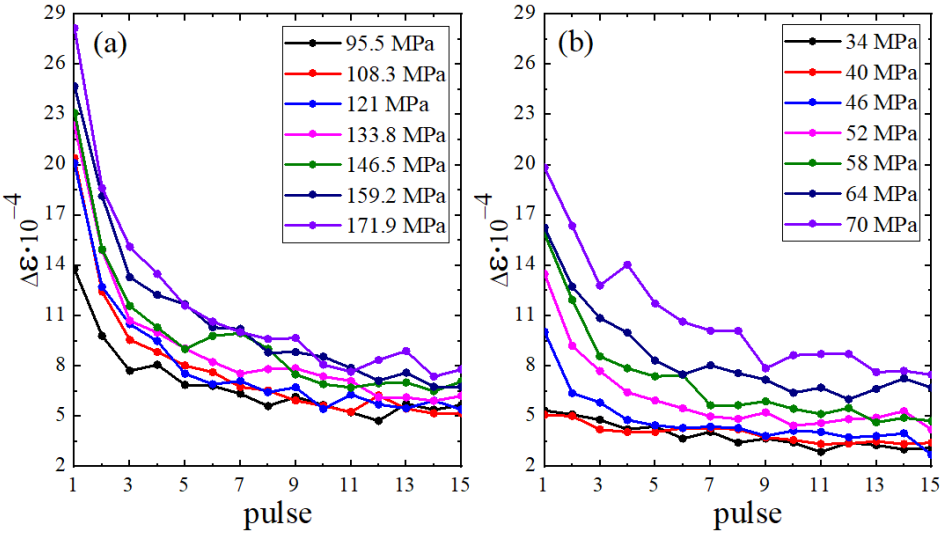

Fig. 10 The increase in plastic deformation as a function of the electric current pulse number at various values of the fixed tensile stress. Fifteen current pulses are applied for each tensile stress, after which the load is increased. Results for the annealed specimens of (a) copper and (b) aluminum. The capacitor bank voltage is 60 V for copper and 75 V for aluminum. The graphs show the average result of two experiments

It can be seen that qualitatively the results do not differ for copper and for aluminum. At tensile stresses below 121 MPa (52 MPa) the effect of electroplasticity is practically not manifested in copper (aluminum), since this stress range is below the flow stress. But with increasing tensile stresses beyond the elastic limit, the effect of electroplasticity is enhanced. The first current pulse gives the largest deformation of the specimen, and with each subsequent pulse this effect becomes weaker until saturation occurs. This can be attributed to the fact that dislocations, whose motion is activated by the current pulse, are gradually fixed on the obstacles or reach the grain boundaries or come to the surface. The fraction of mobile dislocations decreases from pulse to pulse, which leads to a decrease in the plastic strain increment with pulse number.

Figure 10 shows the results of the same experiment but for copper and aluminum wires after annealing. It can be seen that the effect of electroplasticity for the annealed specimens is manifested at lower tensile stresses because their yield strength is lower compared to the specimens in the as-received condition. For the annealed copper wire, the strain due to current pulses increased compared to the as-received wire, see Fig. 9(a) and Fig. 10(a). This is because the metal became more ductile due to the increase in grain size during annealing. However, the same cannot be said for the aluminum specimens. This is due to the fact that aluminum already had rather large grains in as-received state, which grew only slightly as a result of annealing.

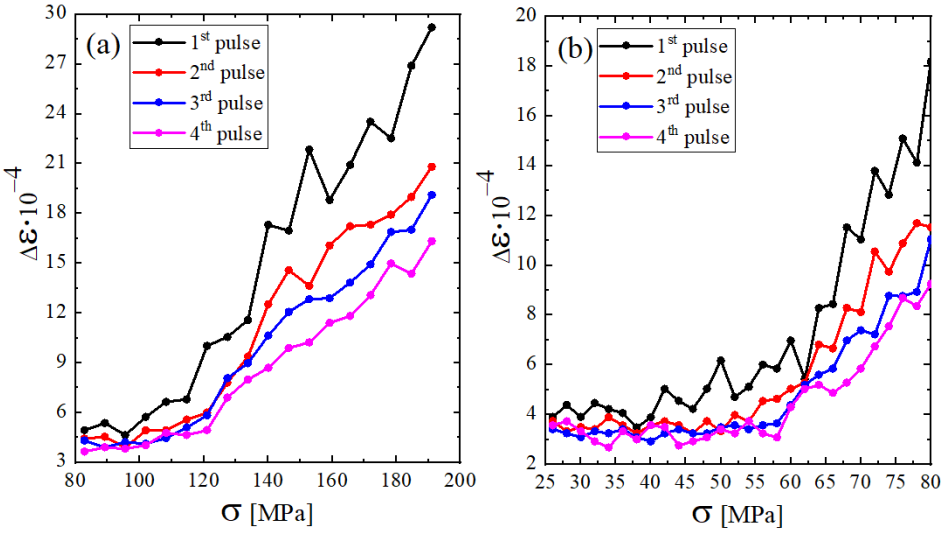

Fig. 11 Increment of plastic deformation as a function of fixed tensile stress for four successive electric current pulses. After every four pulses, the tensile stress increased by about 5%. Results for the as-received specimens of (a) copper and (b) aluminum. The capacitor bank voltage is 60 V for copper and 75 V for aluminum. The graphs show the average result for two experiments

In the next experiment, 4 current pulses were applied at a fixed tensile stress, after which the latter was increased by about 5%. The results for samples in the as-received (annealed) state are shown in Fig. 11 (Fig. 12), where the dependence of strain increment

on tensile stress is plotted in (a) for copper and (b) for aluminum. The black, red, blue and magenta curves denote the first, second, third and fourth current pulses, respectively. It can be seen that regardless of the microstructure of the samples, the dependence revealed in the previous experiment is maintained - the first pulse gives the largest increase in relative elongation, and with each subsequent pulse the strain increment decreases. This is most pronounced for samples after annealing.

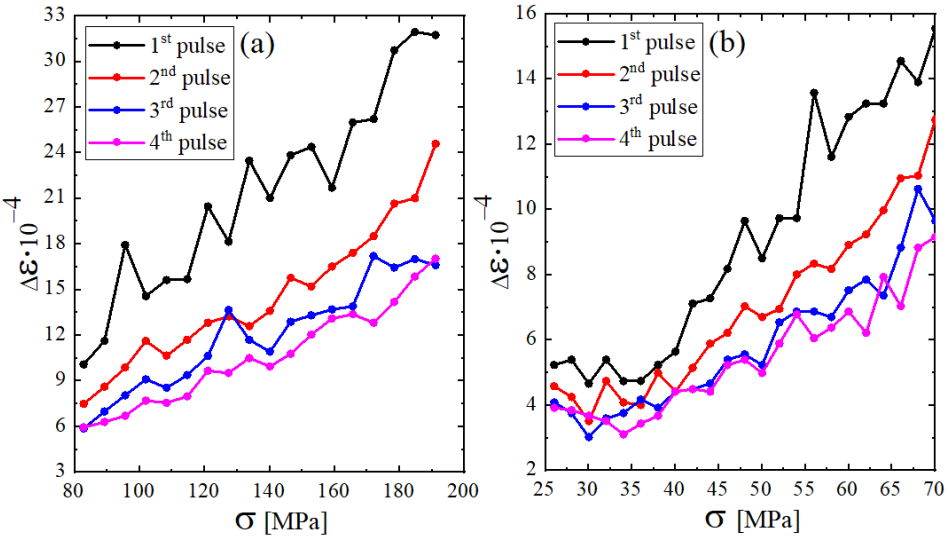

Fig. 12 Increment of plastic deformation as a function of fixed tensile stress for four successive electric current pulses. After every four pulses, the tensile stress increased by about 5%. Results for the annealed specimens of (a) copper and (b) aluminum. The capacitor bank voltage is 60 V for copper and 75 V for aluminum. The graphs show the average result for two experiments

4. CONCLUSIONS

The influence of electric current pulses on plastic deformation of wire samples from M1 grade copper and KAS 8176 grade aluminum in two structural states as-received and after annealing has been investigated.

The heat release on the specimen during pulsed current with different voltages on the capacitor batteries has been evaluated. At capacitor voltages of 60 V for copper and 75 V for aluminum, an increase in sample temperature of 25 K and 17 K was observed, which is 1.84% of the melting point of these metals. The results presented in Figs. 9 through 12 are obtained at these capacitor voltages and, therefore, the observed strain increments during the current pulses of the samples occurred at such a small Joule heating, less than two percent of the melting point. Thus, the classical effect of electroplasticity was observed in this work, when plastic deformation occurs under the action of pulsed current practically without heating the metal. Figures 9 through 12 show that each current pulse causes an increase in strain of the order of 10^{-3}, and it increases with increasing tensile stress and

decreases from pulse to pulse at a fixed tensile stress. If the tensile stress does not exceed the yield stress, the current pulses do not cause elongation of the specimens.

The results for copper and aluminum are qualitatively similar, although the stacking fault energy is significantly different in these two metals. This supports the dislocation mechanism of EE and the presence of numerous twins in copper does not affect the electroplastic deformation. The decrease in wire elongation with pulse number at fixed tensile stress can be explained as follows. Joule heat released mainly on dislocations increases their mobility. While moving, the dislocations reach obstacles or grain boundaries or the specimen surface. The number of mobile dislocations decreases and so does the increment of plastic deformation. However, an increase in tensile stress leads to a resumption of the effect of electroplasticity. The volume-averaged Joule heat release is small because heat is released mainly at defects, particularly dislocations, which are effective scatterers for electrons.

It can be seen from Figs. 9 through 12 that in annealed specimens the plastic deformation caused by electric pulses is somewhat greater than in as-received ones, but the effect of electroplasticity decays faster with the number of pulses due to a smaller number of dislocations. This is clearly seen in the case of copper. In aluminum, however, this effect is barely noticeable due to the insignificant difference in grain size between the as-received and annealed states.

The cooling and creep rates at a fixed tensile stress were also investigated. It was shown that the cooling rate is almost independent of the structural state of the specimen and is 20-50 s for copper wire and 10-50 s for aluminum wire, depending on the capacitor battery voltage. In addition, it was found that creep continues at a slower rate after the specimen has cooled completely.

Our results confirm that the effect of electroplasticity can be used as an energy saving way of metal forming, because the heat is mainly released at dislocations, increasing their mobility and stimulating plastic deformation, while the net Joule heat is small.

Acknowledgement: *This research was supported by the Ministry of Science and Higher Education of the Russian Federation within the framework of the state task of the Ufa University of Science and Technologies (No. 075- 03-2024-123/1) of the youth research laboratory "Metals and Alloys under Extreme Impacts". Kh.G.R. and S.V.D. thank the State Task of Russian Ministry of Science and Education. The electron backscatter diffraction (EBSD) analysis was supported by the program of fundamental researches and it was performed on the equipment of the Center for Shared Access "Structural and Physicomechanical Investigations of Materials" at IMSP RAS.*

REFERENCES

1. Troitskii, O.A., 1969, *Electromechanical effect in metals*, Journal of Experimental and Theoretical Physics Letters, 1(10), pp. 18-22.
2. Okazaki, K., Kagawa, M., Conrad, H., 1978, *A study of the electroplastic effect in metals*, Scripta Metallurgica, 12(11), pp. 1063-1068.
3. Stolyarov, V., Misochenko, A., 2023, *A pulsed current application to the deformation processing of materials*, Materials, 16(18), 6270.
4. Dong, H.-R., Li, X.-Q., Li, Y., Wang, Y.-H., Wang, H.-B., Peng, X.-Y., Li, D.-S., 2022, *A review of electrically assisted heat treatment and forming of aluminum alloy sheet*, International Journal of Advanced Manufacturing Technology, 120(11-12), pp. 7079-7099.
5. Izadpanah, S., Cao, X., An, D., Li, X., Chen, J., 2023, *One step forward to electrically assisted forming mechanisms and computer simulation: A review*, Advanced Engineering Materials, 25(5), 2200425.

6. De Zutter, D., Knockaert, L., 2005, *Skin effect modeling based on a differential surface admittance operator*, IEEE Transactions on Microwave Theory and Techniques, 53(8), pp. 2526-2538.
7. Grimm, T.J., Mears, L.M., 2022, *Skin effects in electrically assisted manufacturing*, Manufacturing Letters, 34, pp. 67-70.
8. Qian, L., Zhan, L., Zhou, B., Zhang, X., Liu, S., Lv, Z., 2021, *Effects of electroplastic rolling on mechanical properties and microstructure of low-carbon martensitic steel*, Materials Science and Engineering: A, 812, 141144.
9. Pochivalov, Yu.I., 2023, *Structure and properties of low-alloy steel 10G2FBYu after rolling in embossed rolls under conditions of electroplasticity*, Izvestiya Ferrous Metallurgy, 66(6), pp. 659-665.
10. Zhan, L., Li, R., Wang, J., Xue, X., Wang, Y., Lv, Z., 2023, *Thermoelectric coupling deep drawing process of ZK60 magnesium alloys*, International Journal of Advanced Manufacturing Technology, 126(7-8), pp. 3005-3014.
11. Tang, G., Zhang, J., Yan, Y., Zhou, H., Fang, W., 2003, *The engineering application of the electroplastic effect in the cold-drawing of stainless steel wire*, Journal of Materials Processing Technology, 137 (1-3 SPEC), pp. 96-99.
12. Lv, Z., Zhou, Y., Zhan, L., Zang, Z., Zhou, B., Qin, S., 2021, *Electrically assisted deep drawing on high-strength steel sheet*, International Journal of Advanced Manufacturing Technology, 112(3-4), pp. 763-773.
13. Yao, K.-F., Wang, J., Zheng, M., Yu, P., Zhang, H., 2001, *A research on electroplastic effects in wire-drawing process of an austenitic stainless steel*, Scripta Materialia, 45(5), pp. 533-539.
14. Li, C., Xu, Z., Peng, L., Lai, X., 2022, *An electric-pulse-assisted stamping process towards springback suppression and precision fabrication of micro channels*, International Journal of Mechanical Sciences, 218, 107081.
15. Wang, Y.-G., He, S.-R., Gu, M., Gao, F., Xiong, K.-H., 2024, *Numerical analysis and springback compensation of metal bipolar plate stamping forming*, Suxing Gongcheng Xuebao/Journal of Plasticity Engineering, 31(2), pp. 43-50.
16. Zhao, L., Chen, G., Liu, J., Wei, H., Huang, J., 2024, *Effect of pulse current parameters on electroplastically assisted dry cutting performance of W93NiFe alloy*, International Journal of Advanced Manufacturing Technology, 131(5-6), pp. 2123-2131.
17. Perkins, T.A., Kronenberger, T.J., Roth, J.T., 2007, *Metallic forging using electrical flow as an alternative to warm/hot working*, Journal of Manufacturing Science and Engineering, 129(1), pp. 84-94.
18. Perkins, T.A., Roth, J.T., 2005, *The reduction of deformation energy and increase in workability of metals through an applied electric current*, American Society of Mechanical Engineers, Manufacturing Engineering Division, MED, 16(1), pp. 313-322.
19. Dong, H., Li, X., Li, Y., Zhao, S., Wang, H., Liu, X., Meng, B., Du, K., 2023, *The anomalous negative electric current sensitivity of a precipitation hardened Al alloy during electrically-assisted forming*, Journal of Materials Research and Technology, 24, pp. 9356-9368.
20. Xu, Z., Jiang, T., Huang, J., Peng, L., Lai, X., Fu, M. W., 2022, *Electroplasticity in electrically-assisted forming: Process phenomena, performances and modeling*, International Journal of Machine Tools and Manufacture, 175, 103871.
21. Tiwari, J., Prasad, K., Krishnaswamy, H., Amirthalingam, M., 2023, *Energy density to explain the ductility loss during electroplastic deformation of a dual-phase steel*, Materials Characterization, 205, 113359.
22. Abdullina, D.U., Bebikhov, Yu.V., Tatarinov, P.S., Dmitriev, S.V., 2023, *Review of recent achievements in the field of electroplastic metal forming*, Basic Problems of Material Science, 20(4), pp. 469-483.
23. Wernicke, S., Hahn, M., Detzel, A., Tillmann, W., Stangier, D., Lopes Dias, N.F., Tekkaya, A.E., 2021, *Force reduction by electrical assistance in incremental sheet-bulk metal forming of gears*, Journal of Materials Processing Technology, 296(48), 117194.
24. Dimitrov, N., Liu, Yu., Horstemeyer, M., 2020, *Electroplasticity: A review of mechanisms in electro-mechanical coupling of ductile metals*, Mechanics of Advanced Materials and Structures, 29(22), pp. 1-12.
25. Kim, M.-J., Yoon, S., Park, S., Jeong, H.-J., Park, J.-W., Kim, K., Jo, J., Heo, T., Hong, S.-T., Cho, S.H., Kwon, Y.-K., Choi, I.-S., Kim, M., Han, H.N., 2020, *Elucidating the origin of electroplasticity in metallic materials*, Applied Materials Today, 21, 100874.
26. Li, X., Zhu, Q., Hong, Y., Zheng, H., Wang, J., Wang, J., Zhang, Z., 2022, *Revealing the pulse-induced electroplasticity by decoupling electron wind force*, Nature Communications, 13(1), 6503.
27. Krishnaswamy, H., Tiwari, J., Amirthalingam, M., 2024, *Revisiting electron-wind effect for electroplasticity: A critical interpretation*, Vacuum, 221, 112937.
28. Li, H., Jin, F., Zhang, M., Ding, J., Bian, T., Li, J., Ma, J., Zhang, L., Wang, Y., 2023, *Decoupling electroplasticity by temporal coordination design of pulse current loading and straining*, Materials Science and Engineering: A, 881(1-3), 145435.

29. Dimitrov, N.K., Liu, Y., Horstemeyer, M.F., 2022, *Electroplasticity: A review of mechanisms in electro-mechanical coupling of ductile metals*, Mechanics of Advanced Materials and Structures, 29(5), pp. 705-716.
30. Hao, S., Chu, Q., Li, W., Yang, X., Zou, Y., 2023, *Effect of electropulsing treatment on the microstructure and mechanical properties of metallic materials: a review, Cailiao Daobao*, Materials Reports, 37(4), 21030039.
31. Liu, J., Jia, D., Fu, Y., Kong, X., Lv, Z., Zeng, E., Gao, Q., 2024, *Electroplasticity effects: from mechanism to application*, International Journal of Advanced Manufacturing Technology, 131(5-6), pp. 3267-3286.
32. Jeong, H.-J., Kim, M.-J., Choi, S.-J., Park, J.-W., Choi, H., Luu, V.T., Hong, S.-T., Han, H.N., 2020, *Microstructure reset-based self-healing method using sub-second electric pulsing for metallic materials*, Applied Materials Today, 20, 100755.
33. Kim, M.-J., Lee, M.-G., Krishnaswamy, H., Hong, S.-T., Choi, I.-S., Kim, D., Oh, K.H., Han, H., 2016, *Electric current–assisted deformation behavior of Al-Mg-Si alloy under uniaxial tension*, International Journal of Plasticity, 94, pp. 148-170.
34. Lahiri, A., Shanthraj, P., Roters, F., 2019, *Understanding the mechanisms of electroplasticity from a crystal plasticity perspective*, Modelling and Simulation in Materials Science and Engineering, 27, 085006.
35. Wang, X., Zhou, B., Huang, H., Niu, J., Guan, S., Yuan, G., 2022, *Extraordinary ductility enhancement of Mg-Nd-Zn-Zr alloy achieved by electropulsing treatment*, Journal of Magnesium and Alloys.
36. Herbst, S., Karsten, E., Gerstein, G., Reschka, S., Nürnberg, F., Zaefferer, S., Maier, H.J., 2023, *Electroplasticity mechanisms in hcp materials*, Advanced Engineering Materials, 25(18), 2201912.
37. Yin, F., Ma, S., Hu, S., Liu, Y., Hua, L., Cheng, G. J., 2023, *Understanding the microstructure evolution and mechanical behavior of titanium alloy during electrically assisted plastic deformation process*, Materials Science and Engineering: A, 869, 144815.
38. Dobras, D., Zimniak, Z., Zwierzchowski, M., Dziubek M., 2024, *Effect of strain rate on the mechanical behavior of Al-Mg alloy under a pulsed electric current*, Metallurgical and Materials Transactions A, 55, pp. 1284-1294.
39. Tiwari, J., Pratheesh, P., Bembalge, O.B., Krishnaswamy, H., Amirthalingam, M., Panigrahi, S.K., 2021, *Microstructure dependent electroplastic effect in AA 6063 alloy and its nanocomposites*, Journal of Materials Research and Technology, 12(3), pp. 2185-2204.
40. Roh, J.-H., Seo, J.-J., Hong, S.-T., Kim, M.-J., Han, H.N., Roth, J.T., 2014, *The mechanical behavior of 5052-H32 aluminum alloys under a pulsed electric current*, International Journal of Plasticity, 58, pp. 84-99.
41. Jeong, H.-J., Park, J.-W., Shin, E., Woo, W., Kim, M.-J., Han, H.N., 2022, *Electric current-induced precipitation hardening in advanced high-strength steel*, Scripta Materialia, 220, 114933.
42. McNeff, P.S., Paul, B.K., 2020, *Electroplasticity effects in Haynes 230*, Journal of Alloys and Compounds, 829(3), 154438.
43. Dong, H., Zhou, H., Li, Y., Li, X., Zhao, S., Liu, X., Wang, Y., 2024, *Temperature-dependent electroplasticity in the Invar 36 alloy*, Journal of Materials Research and Technology, 29(25-26), pp. 3842-3848.
44. Yang, Z., Bao, J., Ding, C., Son, S., Ning, Z., Xu, J., Shan, D., Guo, B., Kim, H.S., 2023, *Electroplasticity in the Al0.6CoCrFeNiMn high entropy alloy subjected to electrically-assisted uniaxial tension*, Journal of Materials Science and Technology, 148, pp. 209-221.
45. Chen, C., Li, C., Li, C., Li, F., Zhang, G., Yu, G., 2022, *Effect of angle between pulse current and load direction on flow stress of Ti-6Al-4V alloy under uniaxial tension*, Journal of Materials Engineering and Performance, 31(11), pp. 9283-9293.
46. Li, X., Hong, Y., Ke, H., Zhong, L., Zou, Y., Wang, J., 2024, *In situ TEM study of pulse-enhanced plasticity of monatomic metallic glasses*, Journal of Materials Science and Technology, 195, pp. 208-217.
47. Li, X., Turner, J., Bustillo, K., Minor, A.M., 2022, *In situ transmission electron microscopy investigation of electroplasticity in single crystal nickel*, Acta Materialia, 223(7), 117461.
48. Kang, W., Beniam, I., Qidwai, S.M., 2016, *In situ electron microscopy studies of electromechanical behavior in metals at the nanoscale using a novel microdevice-based system*, Review of Scientific Instruments, 87(9), 095001.
49. Vu, V.Q., Prokof'eva, O., Toth, L.S., Usov, V., Shkatulyak, N., Estrin, Y., Kulagin, R., Varyukhin, V., Beygelzimer, Y., 2019, *Obtaining hexagon-shaped billets of copper with gradient structure by twist extrusion*, Materials Characterization, 153, pp. 215-223.
50. Beygelzimer, Y., Kulagin, R., Estrin, Y., Toth, L.S., Kim, H.S., Latypov, M.I., 2017, *Twist extrusion as a potent tool for obtaining advanced engineering materials: A Review*, Advanced Engineering Materials, 19(8), 1600873.
51. Xiao, X., Xu, S., Sui, D., Zhang, H., 2021, *The electroplastic effect on the deformation and twinning behavior of AZ31 foils during micro-bending tests*, Materials Letters, 288(7), 129362.

52. Li, X., Xu, Z., Guo, P., Peng, L., Lai, X., 2022, *Electroplasticity mechanism study based on dislocation behavior of Al6061 in tensile process*, Journal of Alloys and Compounds, 910(7), 164890.
53. Bao, J., Chen, W., Bai, J., Xu, J., Shan, D., Guo, B., 2022, *Local softening deformation and phase transformation induced by electric current in electrically-assisted micro-compression of Ti–6Al–4V alloy*, Materials Science and Engineering: A, 831, 142262.
54. Cao, X., An, D., Liu, Q., Chen, G., Li, X., 2024, *Precipitation hardening characterization and stress prediction model in electrically-assisted Ti_2AlNb uniaxial tension*, Intermetallics, 167, 108214.
55. Li, P., Liu, L., Hu, L., Zhang, Y., Yan, S.-L., Xue, K.-M., 2023, *Flow softening rules and mechanisms in Ti–6Al–4V alloy sheet during electrically assisted near-isothermal tension*, Journal of Materials Science, 58(4), pp. 1925-1938.
56. Wu, C., Zhou, Y. J., Liu, B., 2022, *Experimental and simulated investigation of the deformation behavior and microstructural evolution of Ti6554 titanium alloy during an electropulsing-assisted microtension process*, Materials Science and Engineering: A, 838, 142745.
57. Andre, D., Burlet, T., Körkemeyer, F., Gerstein, G., Gibson, J.S.K.-L., Sandlöbes-Haut, S., Korte-Kerzel, S., 2019, *Investigation of the electroplastic effect using nanoindentatio*n, Materials and Design, 183(6), 108153.
58. Zhao Y.H., Liao X.Z., Zhu Y.T., Horita Z., Langdon T.G., 2005, *Influence of stacking fault energy on nanostructure formation under high pressure torsion*, Materials Science and Engineering A, 410-411, pp. 188-193.
59. Muzyk M., Pakiela Z., Kurzydlowski K.J., 2011, *Ab initio calculations of the generalized stacking fault energy in aluminium alloys*, Scripta Materialia, 64(9), pp. 916-918.
60. Hammer B., Jacobsen K.W., Milman V., Payne M.C., 1992, *Stacking fault energies in aluminium*, Journal of Physics: Condensed Matter, 4(50), pp. 10453-10460.
61. Dmitriev S.V., Morkina A.Y., Tarov D.V., Khalikova G.R., Abdullina D.U., Tatarinov P.S., Tatarinov V.P., Semenov A.S., Naimark O.B., Khokhlov A.V., Stolyarov V.V., 2024, *Effect of repetitive high-density current pulses on plastic deformation of copper wires under stepwise loading*, Spectrum of Mechanical Engineering and Operational Research, 1, pp. 27-43.
62. Humphreys, F.J., 2004, *Characterisation of fine-scale microstructures by electron backscatter diffraction (EBSD)*, Scripta Materialia, 51(8), pp. 771-776.